# LAMMPS Framework for Dynamic Bonding and an Application Modeling DNA

Svaneborg, Carsten

*Published in:*
Computer Physics Communications

*DOI:*
10.1016/j.cpc.2012.03.005

*Publication date:*
2012

*Document Version*
Submitted manuscript

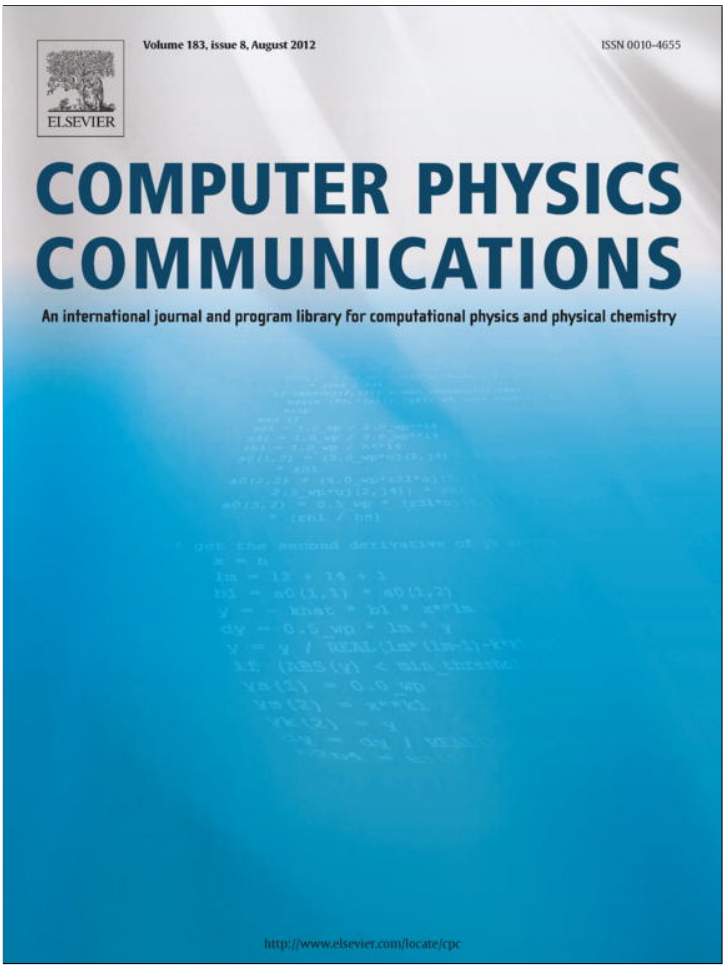

Computer Physics Communications 183 (2012) 1793–1802

Contents lists available at SciVerse ScienceDirect

Computer Physics Communications

www.elsevier.com/locate/cpc

# LAMMPS framework for dynamic bonding and an application modeling DNA ☆

Carsten Svaneborg

*Center for Fundamental Living Technology, Department of Physics, Chemistry, and Pharmacy, University of Southern Denmark, Campusvej 55, DK-5320 Odense, Denmark*

ARTICLE INFO

*Article history:*
Received 21 August 2011
Received in revised form 25 February 2012
Accepted 8 March 2012
Available online 13 March 2012

*Keywords:*
Dynamic directional bonds
Coarse-grain DNA models
Chemical reactions
Molecular and dissipative particle dynamics

ABSTRACT

We have extended the Large-scale Atomic/Molecular Massively Parallel Simulator (LAMMPS) to support directional bonds and dynamic bonding. The framework supports stochastic formation of new bonds, breakage of existing bonds, and conversion between bond types. Bond formation can be controlled to limit the maximal functionality of a bead with respect to various bond types. Concomitant with the bond dynamics, angular and dihedral interactions are dynamically introduced between newly connected triplets and quartets of beads, where the interaction type is determined from the local pattern of bead and bond types. When breaking bonds, all angular and dihedral interactions involving broken bonds are removed. The framework allows chemical reactions to be modeled, and use it to simulate a simplistic, coarse-grained DNA model. The resulting DNA dynamics illustrates the power of the present framework.

**Program summary**

*Program title:* LAMMPS Framework for Directional Dynamic Bonding
*Catalogue identifier:* AEME_v1_0
*Program summary URL:* http://cpc.cs.qub.ac.uk/summaries/AEME_v1_0.html
*Program obtainable from:* CPC Program Library, Queen's University, Belfast, N. Ireland
*Licensing provisions:* GNU General Public Licence
*No. of lines in distributed program, including test data, etc.:* 2 243 491
*No. of bytes in distributed program, including test data, etc.:* 771
*Distribution format:* tar.gz
*Programming language:* C++
*Computer:* Single and multiple core servers
*Operating system:* Linux/Unix/Windows
*Has the code been vectorized or parallelized?:* Yes. The code has been parallelized by the use of MPI directives.
*RAM:* 1 Gb
*Classification:* 16.11, 16.12
*Nature of problem:* Simulating coarse-grain models capable of chemistry e.g. DNA hybridization dynamics.
*Solution method:* Extending LAMMPS to handle dynamic bonding and directional bonds.
*Unusual features:* Allows bonds to be created and broken while angular and dihedral interactions are kept consistent.
*Additional comments:* The distribution file for this program is approximately 36 Mbytes and therefore is not delivered directly when download or E-mail is requested. Instead an html file giving details of how the program can be obtained is sent.
*Running time:* Hours to days. The examples provided in the distribution take just seconds to run.


## 1. Introduction

When performing molecular dynamics simulations, we distinguish between bonded and non-bonded interactions [1,2]. Effectively, this means that the interactions have been coarse-grained on the energy scale of the simulation. Certain degrees of freedom are frozen, and we describe them as being permanent bonded. Other degrees of freedom remain dynamic, and we describe them

☆ This paper and its associated computer program are available via the Computer Physics Communications homepage on ScienceDirect (http://www.sciencedirect.com/science/journal/00104655).

*E-mail address:* science@zqex.dk.

0010-4655/$ – see front matter 
http://dx.doi.org/10.1016/j.cpc.2012.03.005

with relatively weak non-bonded interactions. However, this situation is less clear when simulating systems undergoing chemical reactions where bonds are created or broken. Another example is DNA molecules where hybridization bonds are broken at high temperatures and reformed when cooling the system. For such systems, it can be computationally more efficient to model these degrees of freedom as being dynamically bonded.

The problem of bond dynamics is closely related to the question of how to represent chemical reactions in a molecular dynamics simulation. Reactive force fields such as ReaxFF and empirical valence bond (EVB) can be used to model chemical reactions [3]. Bond order potentials are interesting since they allow three body interactions in the neighborhood of a bond to modify the strength of the bond [4]. When coarse-graining systems capable of chemical reactions, it is important to note that the reaction radius and probability also have to be appropriately coarse-grained [5]. When the bonds become dynamic, this also induces a dynamic for the angular and dihedral interactions. When breaking a bond, all angular and dihedral interactions involving that bond become invalid, and should be removed. Similarly, when creating a bond, we have to identify which angular and dihedral interactions to create in the bond neighborhood. This ensures that after melting and renaturing of a system, it is again governed by the same set of interactions and returns to the same equilibrium structure.

DNA molecules are comprised of the four bases: adenine (A), cytosine (C), guanine (G), and thymine (T). The bases are attached to a 2-deoxyribose sugar ring. For naturally occurring DNA, sugar rings are linked to each other through phosphodiester bonds, that connect the 3′ to 5′ carbons in consecutive sugar rings. This builds a molecular directionality into the backbone of a DNA strand, which will have a 3′ and a 5′ end. The strand is also characterized by a specific sequence of bases. The phosphate backbone, the sugar ring, and the nucleobase are denoted a nucleotide, which is the repeat unit of a single DNA strand. A–T and C–G are Watson–Crick pairs and can form hydrogen bonds with each other. The energetically favorable stacking interactions allow two complementary single strands to form 3′–5′/5′–3′ anti-parallel aligned double strands. Double stranded DNA can be melted and renatured by repeated cycling the temperature around the melting point or by varying solvent conditions.

DNA is a very complex molecule and numerous models exist to describe behavior from atomistic properties to mesoscopic mechanical properties. The molecular structural details of short DNA oligomers can be studied with atomistic molecular dynamics simulations such as Amber [6,7] and Charmm [8,9]. However, when we want to understand the large-scale properties of DNA molecules or materials in which DNA molecules are a component, coarse-grained DNA models are essential. Coarse-graining is the statistical mechanical process by which uninteresting microscopic details are systematically removed, leaving a coarse-grained, effective model that is described by an effective free energy functional [10–13]. A major advantage of coarse-grain models is that we can use them to simulate the interesting large-scale dynamics of a system directly without wasting time on uninteresting details. This allows larger systems to be studied for longer times which paves the way for studying e.g. the properties materials rather than single molecules.

A number of coarse-grain DNA molecular dynamics models exist. In the “three site per nucleotide” model of de Pablo and coworkers, a single nucleotide is represented by a phosphate backbone site, a sugar group site, and a base site, respectively [14–17]. The model uses an implicit representation of counter ions at the level of Debye–Hückel theory, but has recently been generalized to explicit counter ions [18]. A version of this model has also been generalized to include non-Watson–Crick base pairing such as Hoogsteen pairing [19]. There is also a number of “two site per nucleotide” models where one site represents the backbone and the sugar ring. The other site represents the base [20–24]. One challenge to “one site per nucleotide” models is to represent the DNA double helix. Savelyev and Papoian [25,26] do this by special “fan” shaped pair interactions between a bead and a large number of beads on the opposite strand. This model does not allow for DNA melting. Trovato and Tozzini [27] produce a helical structure using angular and dihedral interactions along the double strand. In the case where the large-scale DNA mechanical properties are of interest, it can be advantageous to coarse-grain a whole base pair to a single rigid ellipsoidal or plate-shaped object and regard DNA as a latter-like chain of such objects [28,29]. Here the coarse-graining has eliminated the melting and renaturation dynamics all together. Other types of coarse-grain DNA models are applied to study behavior of DNA functionalized nano-particles. The DNA molecules can e.g. be modeled as rigid rods with a single sticky site on one end and tethered to the surface of the nano-structure by the other end [30], as semi-flexible polymers with attractive sites on the monomers [31], or the whole DNA molecule can be modeled as a single sticky site that can be hybridized to complementary free sticky sites [32]. Here the coarse-graining has completely eliminated the chemical structure, while the melting, renaturing, and sequence specificity have been retained in the dynamics.

The two most prevalent statistical mechanical models of RNA and DNA melting are the Poland–Scheraga [33,34] (PS) and the Dauxois–Peyrard–Bishop [35] (DPB) models. The Poland–Scheraga model describes DNA as a 1D lattice model where a base pair can either be hybridized or open. The free energy expression for the PS model contains empirical stacking free energies each stack of hybridized base pairs as well as contributions from the strand configuration entropy due to internal bubbles, frayed ends and empirical initiation terms. The DPB model also describes DNA as a 1D lattice model, but where each base pair is characterized by a continuous base pair distance. Contrary to the PS model, the DPB model has a Hamiltonian where the base–base potential is described by an anharmonic potential representing hydrogen bonding, and deviations between nearest neighbor base pair extensions are penalized by a harmonic term. A generalization of the PS model exists, where the strand conformations are represented explicitly as lattice polymers. This provides a conceptual simplification since the conformational entropy of bubbles and frayed ends emerge naturally from the polymer model. This real space lattice PS model has been studied using exact enumeration techniques [36], a version of the model has also been applied to study RNA folding using Monte Carlo simulations [37].

The dynamic bonding framework allows us to study classes of DNA models where hybridization bonds, angular bonds, and dihedral bonds are created and broken dynamically. These dynamic bonding DNA models are intermediates between the real space lattice PS models, the coarse-grained molecular dynamics models, and the sticky DNA models described above. In the PS model, base pairs can either be hybridized or open and are characterized by a corresponding free energy. In a dynamic bonding model, base pairs will be either hybridized or open and a free energy will also characterize this transition. In the coarse-grained molecular dynamics models and the DPB model, base pairs are represented by a continuous non-bonded pair-potential. In the dynamic bonding DNA models, base pairs are characterized by a continuous bond potential. The dynamic bond DNA models can also be regarded as being off-lattice generalizations of the real space lattice PS model, where a single strand is described as a semi-flexible bead-spring polymer where complementary monomers will form hybridization bonds when they are close. The dynamic bonded DNA models are “one site per nucleotide” models, but we can also lump sequence of nucleotides into a single coarse-grained bead. In this case, we can as a first approximation assume that only beads representing

complementary sequences can hybridize, and that the breaking of a hybridization bond corresponds to the creation of a DNA bubble. This would be a "many nucleotides per site" dynamic bonding DNA model more akin to the sticky site DNA models used to study DNA functionalized nano-particles.

The dynamic bonded DNA models ensure anti-parallel strand alignment in the double strand state, through the interplay between the dihedral interactions and the directional bonds. Such degrees of freedom are absent from both the PS and DPB 1D lattice models. The coarse-grained models use angular and dihedral interactions to ensure a structure resembling the real chemical structure of DNA molecules. In dynamic bonded DNA models, the angular and dihedral interactions are dynamically introduced when hybridization bonds are formed to promote a zipper-like closing dynamic. Similarly angular and dihedral interactions are dynamically removed as hybridization bonds are broken to promote zipper-like opening dynamic. Hence in dynamic bond DNA model, we utilize the interplay between dynamic bonded, angular, and dihedral interactions to model cooperative effects in the DNA bubble and zippering dynamics, rather than to model chemical structure.

The simplicity and success of the PS model in predicting sequence specific DNA melting temperatures suggests that the essential physics of DNA hybridization, melting and renaturing can, in fact, be accurately captured in a model without chemical details, and where the key property is the dynamics of hybridization. This is our motivation for developing the dynamic bonding framework. We will use it to develop and apply models to study the properties of hybrid materials containing both DNA molecules and soft-condensed matter.

We have implemented directional bonds and dynamic bonding in the Large-scale Atomic/Molecular Massively Parallel Simulator [38] (LAMMPS). LAMMPS is a versatile, parallel, highly optimized, open source code for performing Molecular Dynamics (MD) and Dissipative Particle Dynamics (DPD) simulations of coarse-grained models. Due to the modular design, LAMMPS is easy to extend with new interactions and functionality. The dynamic bonding implementation is also modular and easy to extend with new functionality. Our extension is by no means limited to modeling DNA, but could equally well be used for simulations of chemical reactions such as living polymerization, cross-linking of stiff polymers, coarse-grained dynamics of worm-like micelles and active driven materials. A snapshot of the LAMMPS code with the directional bonds and dynamic bonding implementation can be obtained from the CPC Program Library. Included with the code is also the documentation necessary for porting the directional and dynamic bonding framework to future LAMMPS versions.

Section 2 is a summary of the implementation of directional bonds and the dynamic bonding framework. We present a simplified DNA model based on the dynamic bonding framework in Section 3, which provides the examples of DNA dynamics shown in Section 4. We conclude with our conclusions in Section 5, and present the details of the directional bonds and dynamic bonding implementation in Appendix A.

## 2. Implementation

Double stranded DNA only exists in a state where the two strands are aligned anti-parallel 3′–5′/5′–3′. In order to distinguish between parallel and anti-parallel strand alignment, we regard the 3′–5′ backbone structure as a property of the backbone bonds, which become directional. This is necessary since the chemical structure of the nucleotides has been coarse-grained to a single structureless site. The directional bonds will also play a crucial role when introducing angular and dihedral interactions in a double stranded DNA molecule, since this affects the stability, zippering dynamics, and mechanical properties.

To implement directional bonds in LAMMPS, we make use of the fact that Newton's 3rd law is optional when calculating bond forces. When Newton's 3rd law is enabled, each bond force is only calculated once, but subsequently has to be communicated to the bond partner. When it is disabled, LAMMPS calculates the bond force twice, once for each of the two bond partners. In this case, each of the two bond partners store information about the bond type and the identity of the other bond partner. We can denote this situation by $A \xrightarrow{t} B$ and $A \xleftarrow{t} B$, which shows that the $A$ bead stores $t$ as the type of the bond to $B$, and the $B$ bead stores $t$ as the type of the bond to $A$. With a few modifications, LAMMPS will load and store different bond types in the two bond partners. Hence, we can have $A \xrightarrow{t} B$ and $A \xleftarrow{s} B$, where the bond type $s$ from $B$ to $A$ and the bond type $t$ from $A$ to $B$ differ. When the two bond types refer to the same bond potential, Newton's 3rd law still applies, and the dynamics is unaffected. However, we can interpret the pattern of bond types as the directionality of the strand. Note that if we instead use different bond potentials in the two directions or only a "half" bond, the result would be a net force along the bond, which can be used to model driven active matter. We shall not pursue this situation further in the present paper.

The dynamic bonding framework allows a number of rules to be specified, that completely define the bond dynamics. These rules are applied to a specified group of reactive beads with a specified frequency. The application of the rules is conditional on the types of beads, types bonds, distance between beads and length of bonds involved. In particular, we have implemented rules for stochastic creation of symmetric and directional bonds within a certain reaction distance, stochastic removal of symmetric bonds larger than a breaking distance, removal of all symmetric bonds exceeding a certain length, and stochastic conversion of a symmetric bond from one type to another. Furthermore, all bond creation rules ensure that a bead can never have more than a specified number of bonds of a given type. The implementation is structured such that it is easy to implement new types of rules.

Besides the bond dynamics, the consistency of the angular and dihedral interactions should be ensured at all times. After bonds have been broken, all invalid potential angular and dihedral interactions involving broken bonds should also be removed. After bonds have been formed, all triplets or quartets of beads that could be connected by at least one new bond are checked to see if they require the creation of an angular or dihedral interaction. We discard cyclic triplets and quartets where the same bead appears more than once.

An angular creation rule specifies which angular interaction can be introduced between a triplet of connected beads $A$, $B$, and $C$. Since the triplets are not ordered, the rule should match either *ABC* or *CBA*. To test if the *ABC* bead order matches, we first compare the types of the *ABC* beads with the bead types the rule specifies. We then compare the two bond types $t$ and $s$ with the bond types the rule specifies, where the bond types are defined directionally as $A \xleftarrow{t} B$ and $B \xrightarrow{s} C$. If the *ABC* bead order did not match, it is repeated *CBA* bead order, where the bonds types are defined directionally as $C \xleftarrow{t} B$ and $B \xrightarrow{s} A$. If a rule matches, then the specified angular interaction is introduced between the three beads. A creation rule for a dihedral interaction specifies four bead types and three bond types. Again we test both *ABCD* and *DCBA* ordered bead quartets. First the bead types of the quartet are compared to the bead types specified by the rule, subsequently the bond types are compared, the bond types are defined directionally as $A \xleftarrow{r} B$, $B \xleftarrow{s} C$, $B \xrightarrow{s'} C$, and $C \xrightarrow{t} D$. The bond types match if $r$, $s$ or $s'$, and $t$ match the three bond types specified by the rule. If the *ABCD* bead order did not match, it is repeated *DCBA* order. If a

Define a dynamic bond fix:
FIX fixid beadgroup BONDDYNAMICS *everystep* [PAIRCHECK13] [PAIRCHECK14]
<list of rules>

Each dynamic bonding rule is one of:
CREATEBOND *bondtype beadtype1 beadtype2* maxdistance probability
CREATEDIRBOND *bondtype1 bondtype2 beadtype1 beadtype2* maxdistance probability
BREAKBOND bondtype mindistance probability
CONVERTBOND bondtype1 bondtype 2 probability
KILLBOND *bondtype* mindistance
CREATEANGLE *angletype beadtype1 beadtype2 beadtype3 bondtype1 bondtype2*
CREATEDIHEDRAL *dihedraltype beadtype1 beadtype2 beadtype3 beadtype4 bondtype1 bondtype2 bondtype3*
MAXBOND *bondtype beadtype maxnumber*

**Fig. 1.** LAMMPS syntax for the dynamic bonding fix, and the types of rules currently implemented.

dihedral rule matches a quartet of beads, the specified dihedral interaction is introduced between the four beads. These rules allow us to selectively and dynamically introduce angular and dihedral interactions taking both bead types and directional bond types into account. Note that the same directionality applies to matching the bead type and bond type patterns.

To have an efficient parallel implementation, we implement the bond creation and breaking by a pair matching algorithm inspired from the bond/break and bond/create fixes already implemented in LAMMPS. In the dynamic bonding fix, preferred bond creation/breakage partners are identified in each simulation domain. This information is communicated between and aggregated across neighbor simulation domains. Afterwards, the bonds selected for breakage are removed. The local neighborhood of all reactive beads are checked for angular and dihedral interactions, that should be removed because they cross broken bonds. Then bonds are created between partners selected for bonding. Again, we check the local neighborhood of all reactive beads to introduce angular and dihedral interactions. After this final step, we broadcast bond statistics to all simulation domains. Note that due to the pair matching algorithm, each bead can maximally have one bond created and broken at each call to the dynamic bonding fix. All rules are applied to a bead pair (in the specified order) when identifying if they are eligible for matching. If multiple rules apply to the same bead pair, the last matching rule will always be chosen. Hence, if this last rule has a very low reaction probability, it will completely shadow more probable rules specified earlier. These shadowing issues do not apply to the DNA model below, and will not play a role at low concentrations of reacting beads. The details of the implementation and shadowing issues are discussed in Appendix A, 6.

The LAMMPS syntax of the dynamic bond fix is shown in Fig. 1. The first line defines the name of the particular instance of the fix, the group of reactive beads (*beadgroup*), and how often the bond dynamics fix is applied (*everystep*). By default creation rules only apply to potential bonding bead pairs, that are further than 4 bonds apart or not bonded. The optional *Paircheck13* and *Paircheck14* switches include 1–3 and 1–4 chemically distant beads in the search of potential bonding partners. The line is followed by a number of dynamic bonding rules. *Createbond* rules specify pairs of bead types, that can be bonded, if they are within a certain maximum reaction distance from each other. If a bead has more than one potential bond partners, the closest partner is chosen, and a bond with the specified type is then created with the given probability. *Createdirbond* rules do the same as *createbond*, but create a directional bond with the two specified bond types between the two bead types. *Breakbond* rules identify bonded bead pairs with bonds longer than the specified minimum distance and break the bond with the specified probability. If a bead has more than one potential bond break partner, then the most distant partner is chosen. Since only a single bond can be removed per bead per call to the dynamic bonding fix, a breakbond rule with unit probability does not ensure that all bonds longer than the minimum distance are broken. Hence, we have also implemented *killbond* rules. These rules operate directly on the bond structures, and are not limited by the pair matching algorithm. *Convertbond* rules stochastically convert symmetric bonds of one type into another type. This is implemented as nominating the bond pair for removal of the old bond, followed by creation of the new bond. The dynamic bonding framework ensures that angular and dihedral interactions across the bond are also converted accordingly. *Createangle* and *Createdihedral* rules define which angular and dihedral interaction types should be created between triplets and quartets of beads with the specified types of bead, and types of bonds between the beads as discussed above. *Createangle* and *createdihedral* rules do not specify a probability, since they are created as required by the local neighborhood around new bonds. Note that angular and dihedral interactions are only introduced as a consequence bond creation events, they are not introduced between already bonded beads even though the bead types and bond types match the rule. When checking potential beads for bond creation, all *Maxbond* rules are checked to discard beads that already have the maximal number of the specified bond types.

## 3. DNA model

We have chosen the present DNA model because it produces a simple ladder like equilibrium structure, which allows us to illustrate the power of the dynamic bonding framework, and to visualize all the interactions that are dynamically introduced and removed. Real DNA molecules perform a whole twist every 10.45 base pairs, and to model the twist we need a somewhat more complex force field, but exactly the same dynamic bonding rules. Because we are interested in studying DNA programmed self-assembly, we choose to use Dissipative Particle Dynamics (DPD) [39,40]. DPD is given by a force field comprising a conservative soft pair-force $F^C$, a dissipative friction force $F^D$, and a stochastic driving force $F^R$ given by

$$\mathbf{F}_{ij} = \left(F^C + F^R + F^D\right)\frac{\mathbf{r}_{ij}}{r} \quad \text{for } r = |\mathbf{r}_{ij}| < r_c$$

where the forces contributions are given by

$$F^C = a\,w(r), \qquad F^D = -\frac{\gamma\, w^2(r)}{r}(\mathbf{r}_{ij}\cdot\mathbf{v}_{ij}), \qquad F^R = \frac{\sigma\, w(r)\xi}{\sqrt{\Delta t}}.$$

Here $\mathbf{r}_{ij} = \mathbf{r}_i - \mathbf{r}_j$ and $\mathbf{v}_{ij} = \mathbf{v}_i - \mathbf{v}_j$ denote the separation and relative velocity between two interacting beads $i$ and $j$, respectively. $\xi$ denotes a Gaussian random number with zero mean and unit variance, and the thermostat coupling strength is $\sigma = \sqrt{2k_BT\gamma}$. The

```
1: fix dnadyn dna bonddynamics 1 paircheck14
2: CREATEBOND 1 1 2 0.6 1.0
3: CREATEBOND 1 3 4 0.6 1.0
4: CREATEDIRBOND 2 3 2 3 0.3 0.1
5: KILLBOND 1 1.0
6: MAXBOND 1 * 1
7: MAXBOND 1 * 2
8: MAXBOND 1 * 3
9: CREATEANGLE 1 * * * 2 3
10: CREATEANGLE 2 * * * 1 2,3
11: CREATEDIHEDRAL 1 * * * * 1 2,3 1
12: CREATEDIHEDRAL 2 * * * * 2 1 3
13: CREATEDIHEDRAL 3 * * * * 2 1 2
14: CREATEDIHEDRAL 3 * * * * 3 1 3
```

**Fig. 2.** LAMMPS dynamic bonding fix for producing the DNA dynamics shown in Figs. 3–7. Bond types are shown with plain digits (hybridization: red 1, backbone 3′ bonds: green 2, and backbone 5′ bonds: blue 3). Bead types are shown with bold digits representing nucleotides (A: red 1, T: green 2, C: blue 3, G: magenta 4). Angular and dihedral bond types are shown with italic digits corresponding to the interaction type numbers. The bead and interaction type colors correspond to those used in the visualizations. $*$ is the wild card and is used to match any bead or bond type. (For interpretation of the references to color in this figure, the reader is referred to the web version of this article.)

weighting function is $w(r) = 1 - \frac{r}{r_c}$. We integrate the DPD dynamics with a Velocity Verlet algorithm with a time step $\Delta t = 0.01\tau$. The unit of energy is $\epsilon = k_B T$, where we chose to set Boltzmann's constant to unity, such that temperature is measured in energy units. We use $T = 1\epsilon$ in all of the simulations except the DNA bubble simulation where $T = 5\epsilon$. The unit of length $\sigma$ is defined by the pair-force cut-off $r_c = 1\sigma$. The mass is $m = 1$ for all beads, this allows us to define the unit of time as $\tau = \sigma\sqrt{m/\epsilon}$. The DPD pair-force parameter is $a = 25\epsilon\sigma^{-1}$ between all species of beads. The viscosity is $\eta = 100\epsilon\tau\sigma^{-2}$. Non-bonded pair interactions are switched off between beads in molecules that are less than 3 bonds apart. The DNA molecule is simulated in an explicit solvent at a density $\rho = 3\sigma^{-3}$.

We represent a nucleotide by a single DPD bead, and let the four ATCG nucleotides correspond to bead types 1–4, respectively. They are colored red, green, blue, and magenta, respectively, in figures below. Red and green beads (A–T) are complementary as are blue and magenta (C–G) beads. A single strand of DNA is represented as a string of beads joined by permanent directional backbone bonds. The two 3′ to 5′ and 5′ to 3′ backbone bond potentials (bond type 2 and 3, respectively, colored green and blue in the bond visualizations) are given by the same potential

$$U_{backbone}(r) = \frac{U_{\min}}{(r_l - r_0)^2}\left((r - r_l)^2 - (r_0 - r_l)^{-2}\right),$$

with $U_{\min} = 10.0\epsilon$, $r_l = 0.3\sigma$, and $r_0 = 0.6\sigma$. The hybridization bond potential (bond type 1, colored red in the bond visualizations) is given by

$$U_{hyb}(r) = \begin{cases} \frac{U_{\min}}{(r_h - r_0)^2}\left((r - r_0)^2 - (r_h - r_0)^{-2}\right) & \text{for } r < r_c, \\ 0 & \text{for } r \geqslant r_c \end{cases}$$

with $U_{\min} = 1.0\epsilon$, $r_h = 0.6\sigma$, and $r_c = 1.0\sigma$.

Besides the DNA interactions, we need to define the bonding dynamics of the DNA beads. The corresponding dynamic bonding fix command is shown in Fig. 2. Hybridization bonds are created with probability one when two complementary beads are within a distance of $r_h$. Bead type 2 and 3 are able to form a 5′ 3′ backbone bond when they are within a distance of $r_l = 0.3\sigma$ from each other. The probability of creation of a backbone bond is 0.1. This is a simplification for the oligomer-template simulation below. Only hybridization bonds can be broken, and they are removed if they are longer than $r_c = 1\sigma$. To control hybridization, we only allow all bead types ($*$) to have maximally one hybridization bond (type 1), one 3′ end (type 2) and one 5′ end (type 2) of a backbone bond. In the model all nucleotides have the same interactions, hence use $*$ for all the bead types rule specifications.

The model has two angular interactions, which are described by the potential $U(\theta) = K(\theta - \theta_0)^2$, where $K$ defines the angular spring constant and $\theta_0$ the equilibrium angle. The first angle interaction (type 1) promotes a straight angle between backbone bonds. This interaction is shown as red angles in the angle visualizations, and it has parameters $K = 20\epsilon$ and $\theta_0 = 180$. Type 1 angles are dynamically introduced for bonding patterns $A \overset{3'}{\leftarrow} B$, $B \overset{5'}{\rightarrow} C$ and $A \overset{5'}{\leftarrow} B$, $B \overset{3'}{\rightarrow} C$ (i.e. for model bonds types 2 3, since *CBA* order matches 3 2). The second angle interaction (type 2) promotes a right angle between backbone and hybridization bonds. This interaction is shown as green angles in the angle visualizations, and it has $K = 1\epsilon$ and $\theta_0 = 90$. Type 2 angles are dynamically introduced for bonding patterns $A \overset{H}{\leftarrow} B$, $B \overset{3'/5'}{\rightarrow} C$ and $A \overset{3'/5'}{\leftarrow} B$, $B \overset{H}{\rightarrow} C$ (i.e. model bond types 1 and 2, 3, since *CBA* order matches the reverse pattern).

The DNA model has three dihedral interactions, which are described by the potential $U(\phi) = K(1 + d\cos(\phi))$. We use dihedral spring constant $K = 1.0\epsilon$, and $d = +1$ $(-1)$ for promoting trans (cis) conformations. The first dihedral interaction (type 1, shown red in dihedral visualizations) promotes a cis conformation when a backbone bond connects two hybridized nucleotide pairs. This corresponds to the bonding patterns $A \overset{H}{\leftarrow} B$, $B \overset{3'}{\leftarrow} C$, $B \overset{5'}{\rightarrow} C$, $C \overset{H}{\rightarrow} D$ and $A \overset{H}{\leftarrow} B$, $B \overset{5'}{\leftarrow} C$, $B \overset{3'}{\rightarrow} C$, $C \overset{H}{\rightarrow} D$, where $H$ denotes a hybridization bond (i.e. model bond numbers 1 2, 3 1). The second dihedral interaction (type 2, shown green in the dihedral visualizations) promotes a cis conformation of the two beads that are connected by backbone bonds to a hybridized bead pair and is located on the same side of the bead pair. The bonding pattern is $A \overset{3'}{\leftarrow} B$, $B \overset{H}{\leftarrow} C$, $B \overset{H}{\rightarrow} C$, $C \overset{5'}{\rightarrow} D$ (i.e. model bond numbers 2 1 3). The third interaction (type 3, shown blue in the dihedral visualizations) promotes a trans conformation of the two bead that are connected by backbone bonds to a hybridized bead pair but are localized on opposite sides of the bead pair. The bonding patterns are $A \overset{3'}{\leftarrow} B$, $B \overset{H}{\leftarrow} C$, $B \overset{H}{\rightarrow} C$, $C \overset{3'}{\rightarrow} D$ and $A \overset{5'}{\leftarrow} B$, $B \overset{H}{\leftarrow} C$, $B \overset{H}{\rightarrow} C$, $C \overset{5'}{\rightarrow} D$ (i.e. model bond numbers 2 1 2 and 3 1 3). Note that without the directional bond, we would be unable to distinguish between these two last types of dihedrals. The examples below are included as test cases with the dynamic bonding code submitted to the CPC Program Library, and require less than a CPU hour of computational effort.

## 4. Example DNA dynamic

To illustrate the dynamic bonding framework with the DNA model, we simulate a $5' - ATCGATCG - 3'$ template in the presence of two $3' - TAGC - 5'$ oligomers. The first oligomer is already hybridized with the template, while the second is placed in the vicinity of the template. Fig. 3 shows snapshots along the trajectory where the remaining oligomer hybridizes with the template. The top left visualization shows the initial designed configuration. The blue–green pattern of the hybridized oligomer backbone shows it has 3′ 5′ direction, while the green–blue pattern of the template backbone shows the 5′ 3′ direction. The top center visualization shows the angular interactions of the initial configuration. The backbone stiffness is controlled by the red angular interactions between backbone bond pairs, which promote a straight backbone configuration. The green angular interactions promote hybridization bonds that are perpendicular to the strand axis. The

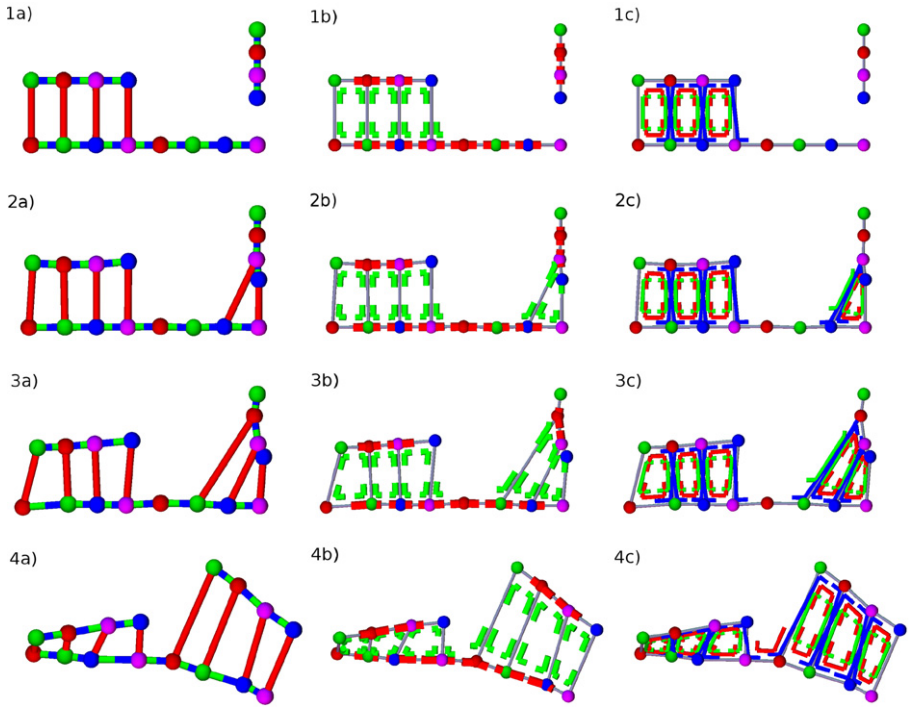


**Fig. 3.** Oligomer – DNA template hybridization (rows 1–4) showing the dynamics of bond, angular, and dihedral interactions (columns a–c) for times $t = 0$, $0.01\tau$, $0.04\tau$, and $0.23\tau$ into the simulation. Bead and interaction colors match those in Fig. 2. Note that backbone bond directionality is only shown in the first row for simplicity. (For interpretation of the references to color in this figure, the reader is referred to the web version of this article.)

top right visualization shows the dihedral interactions of the initial configuration. The hybridized template shows red and green dihedral interactions which promote cis arrangement of stacked bead pairs, while the blue dihedral interaction promotes trans arrangement. Together they stabilize the ladder-like structure of the double strand. Without the bond directionality, we would have no way to distinguish between green and blue dihedral interactions, and hence control over the stiffness of the double strand relative to that of the single strands.

As we let the simulation run (left column top to bottom) initially two hybridization bonds are introduced between the two beads at right most end of the template. Later a third and a fourth hybridization bond are also introduced. Along with the hybridization bonding dynamics, angular and dihedral interactions (center and right columns) are also created. The angular interactions cause the free oligomer to align with the template, while the dihedral interactions create a torque that ensures that the alignment is anti-parallel.

Fig. 4 shows how the nick in the DNA molecule is closed by forming a backbone bond. The interactions between the two oligomers and the template ensure that they are both aligned anti-parallel to the template backbone axis. The single red dihedral interaction across the nick promotes a cis configuration, and twists the two oligomers towards the same side of the template. Finally the missing backbone bond is created following the 3′–5′ directionality of the strand, along with all the angular and dihedral interactions to produce a double stranded configuration. Together Figs. 3 and 4 simulate a chemical reaction where a DNA template and two complementary oligomers first hybridize due to their complementary sequences, and then ligate to produce the complementary template sequence.

To melt the double strand, we can e.g. apply an external force to tear the two strands apart [41] or increase the temperature to let thermal fluctuations do the work. Fig. 5 shows the result of applying an external opposing force to left most nucleotide pair. Progressively the left most hybridization bond snaps. Along with the breakage of hybridization bonds, we also see the gradual removal of green angular interactions and all the dihedral interactions. The external force is opposed by a single left most hybridization bond along with the angular and dihedral interactions across the gab. During the unzipping process, often the hybridization bonds are transiently reformed just after breakage if thermal fluctuations pull them within the hybridization reaction distance.

In Fig. 6 we perform another pulling experiment, where a much stronger horizontal force is applied to the left most bottom strand and right most top strand beads of the double strand. Initially the whole molecule is sheared, as all the green angular interactions cooperate in opposing the deformation. Gradually bonds snap from either end towards the center. Interestingly, since the two molecules have a 4-nucleotide long repeating sequence, when the hybridization bonds are broken, they very rapidly reform with the complementary beads one repeat sequence further down the molecule. The shear process repeats for the second hybridization sequence until it too is broken, and two single strands are formed.

DNA can be molten by raising the temperature. The melting temperature depends on the sequence, the length of the strands as well as the strand concentration [33,42]. Prior to melting, bubbles of open nucleotide sequences appear since they contribute configuration entropy and hence lower the free energy similar to vacancies in crystals. At increased temperatures, the number and the size of these bubbles grow and cause the two strands to melt [43–46]. In Fig. 7 we show a time series of a bubble, that is created by breaking a single hybridization bond, the bubble grows until it breaks the last hybridization bond. However, the two frayed strands form a hybridization bond at the end, and progressively the bubble closes again. Simulating the chain for sufficiently long time at an elevated temperature will cause the double strands to melt with a transition very much like the one shown in Fig. 7.

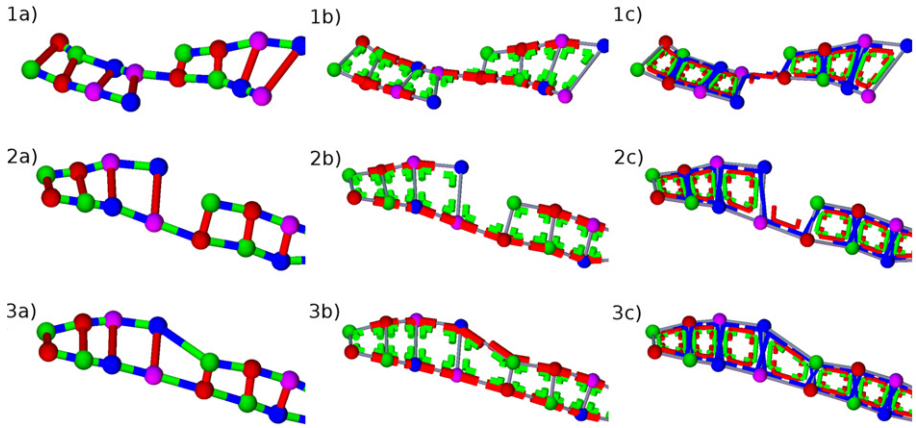


**Fig. 4.** Backbone ligation reaction by addition of directional backbone bond (rows 1–3) showing dynamic of bond, angular and dihedral interactions (columns a–c) for the simulation in Fig. 3 continued to times $11.50\tau$, $12.46\tau$, and $12.48\tau$, respectively. (For interpretation of the references to color in this figure, the reader is referred to the web version of this article.)

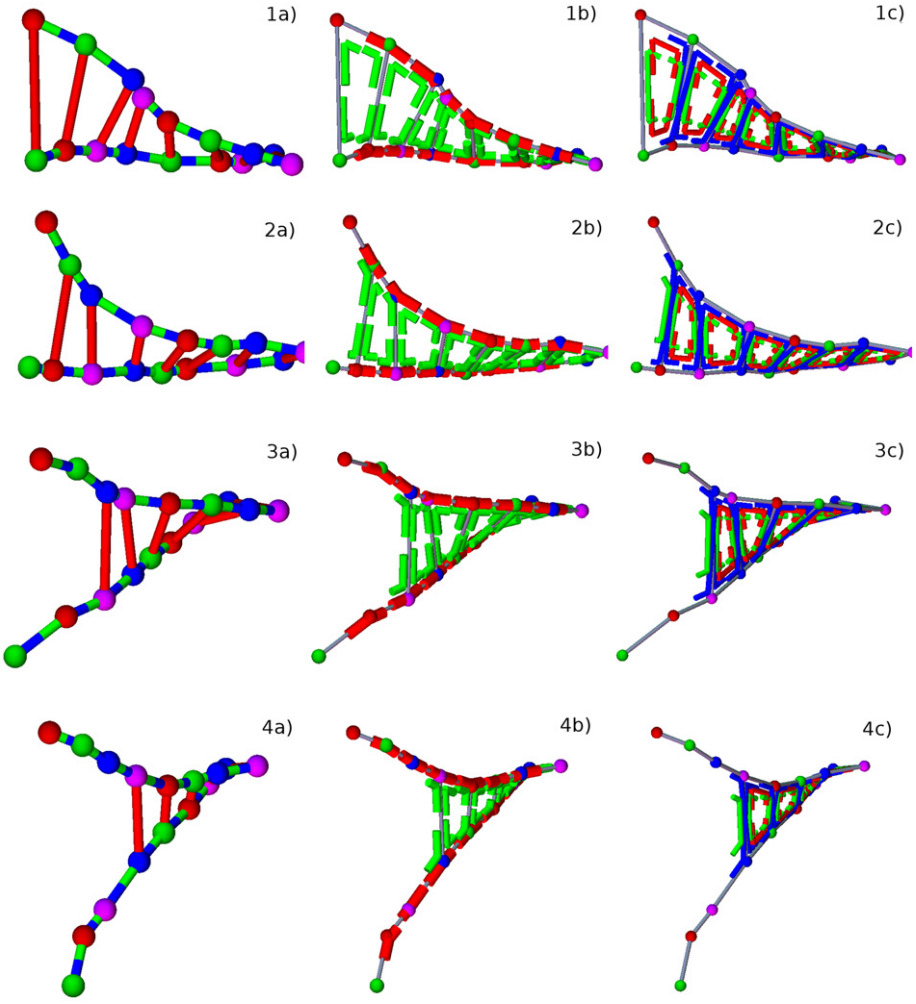


**Fig. 5.** DNA unzipping by a weak vertical force $f = 28\epsilon\sigma^{-1}$ applied to the left most bead pair (rows 1–4) for bond, angular and dihedral interactions (columns a–c). The rows correspond to times $1.72\tau$, $1.84\tau$, $3.03\tau$, $3.22\tau$, respectively, starting from a straight double strand conformation at $t = 0\tau$. (For interpretation of the references to color in this figure, the reader is referred to the web version of this article.)

## 5. Conclusions

We have implemented a versatile framework for studying the effects of dynamic bonding of ordinary and directional bonds in coarse-grained models within the context of the Large-scale Atomic/Molecular Massively Parallel Simulator (LAMMPS) [38]. The dynamic bonding framework ensures that angular and dihedral interactions are kept consistent during bond breakage and creation. The code has been parallelized and optimized to the case where the bond formation or breakage probability for each bead is relatively low. Since the dynamic bonding code is very modular it will be easy to extend with other types of bonding rules. The dynamic

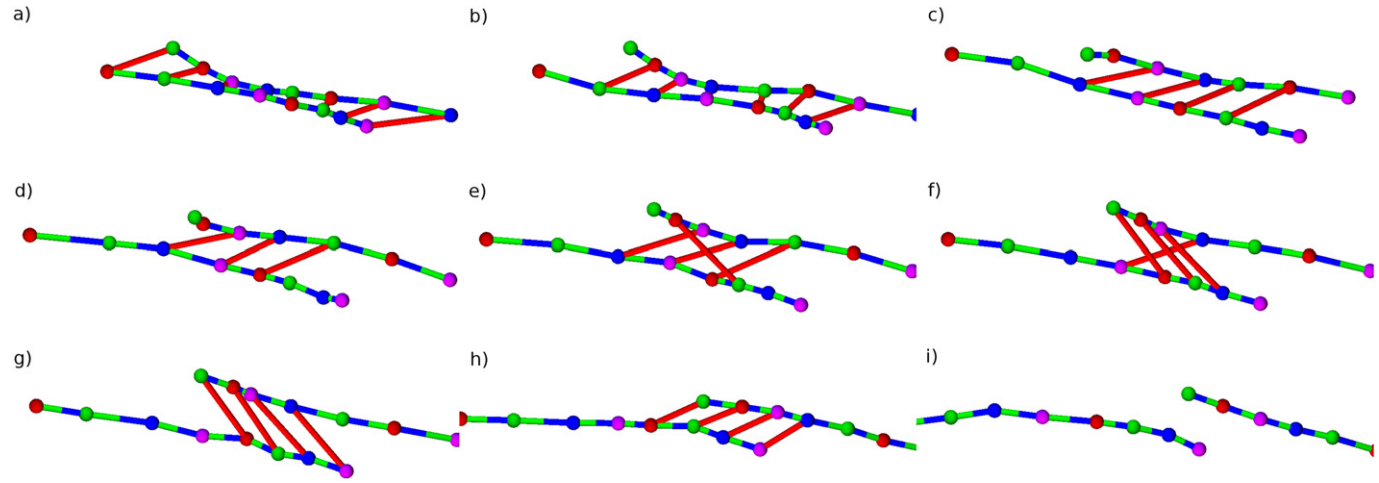


**Fig. 6.** Time series of DNA unzipping by a strong horizontal force $f = 100\epsilon\sigma^{-1}$ applied to the left and right most beads of the two strands (a–h). The snapshots correspond to times $0.21\tau$, $0.30\tau$, $0.59\tau$ (top row), $0.81\tau$, $0.89\tau$, $0.92\tau$ (middle row), and $0.95\tau$, $1.20\tau$, $1.37\tau$ (bottom row) starting from a straight double stranded conformation at $t = 0\tau$. (For interpretation of the references to color in this figure, the reader is referred to the web version of this article.)

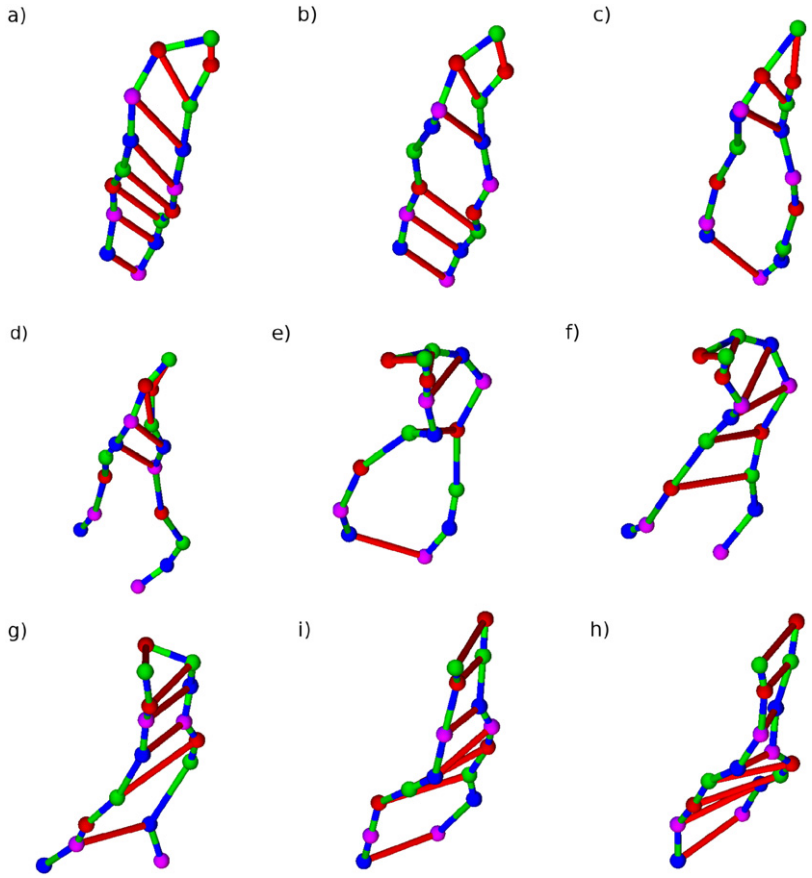


**Fig. 7.** Time series showing bubble opening and closing dynamics for DNA at an elevated temperature $T = 5\epsilon$ (a–h). The snapshots are from times $t = 55.40\tau$, $55.44\tau$, $55.48\tau$ (top row), $55.55\tau$, $55.85\tau$, $55.89\tau$ (middle row), and $55.96\tau$, $56.05\tau$, $56.09\tau$ (bottom row) starting from a straight double stranded conformation at $t = 0\tau$. (For interpretation of the references to color in this figure, the reader is referred to the web version of this article.)

bonding framework was written with the aim of developing a new type of coarse-grained models of DNA dynamics. We have illustrated a dynamic bonding DNA model using DNA hybridization and ligation, as well as two geometries of force induced unzipping and bubble dynamics. Clearly the present DNA model is very simple, nonetheless it qualitatively captures some of the fundamental phenomena of DNA molecules. The dynamic bonding framework will allow us to build DNA models, that we expect will provide quantitative predictions as good as the Poland–Scheraga model [33,34], while we can use these DNA models as components in Molecular Dynamics and Dissipative Particle Dynamics simulations of hybrid materials containing both soft-condensed matter and DNA molecules.

## Acknowledgements

C.S. gratefully acknowledges discussions with H. Fellermann, R. Everaers, P.-A. Monnard, M. Hanczyc, and S. Rasmussen.

The research leading to these results has received funding from the European Community's Seventh Framework Programme (FP7/2007–2013) under grant agreement no. 249032. Funding for this work is provided in part by the Danish National Research Foundation through the Center for Fundamental Living Technology (FLinT).

## Appendix A. Implementation details

When Newton's 3rd law is not applied to bonded interactions, LAMMPS has a bond interaction table for each bead listing the other beads it is bonded to and the type of the bond. Similar angular and dihedral interaction tables exist for each bead. LAMMPS also has a neighbor structure where bonded neighbors, next nearest neighbors, and third nearest neighbors are stored. This information is derived from the bonding structure, and used to enable or disable non-bonded interactions between beads connected by up to three bonds.

Initially when LAMMPS reads the control file to set up a simulation, the dynamic bonding fix is called to parse the entire set of rules such as those in Fig. 2. The rules and their parameters are sanity checked and stored internally in the fix. When the simulation is initialized, the dynamic bonding framework starts by having each simulation domain count how many bonds of each type each reactive bead has.

Then at a specified frequency the code does:

1. Communication. Forward communication of ghost particle positions to neighboring nodes and the table of bond counts. This is required for testing distances and for applying maximum rules.
2. Creation nomination. Each reactive bead can nominate a single preferred bonding partner. The search for partners is performed over all beads in the reactive group and each creation rule is tested in succession. The test of rules is done in the order they are specified, and if more than one rule match the same bead pair, the last matching rule will apply. The search is over all non-bonded beads and optionally over beads 2 or 3 bonds away from the current bead. For each bead pair and creation rule, their types are tested and if they within the maximum reaction distance. Beads that already have the maximal number of bonds of the type, that would be produced by the current rule are discarded. Of all the potential bonding partners, the closest partner in the same simulation domain (if any) is nominated for bonding.
3. Bond breakage nomination. Each reactive bead can nominate a single preferred partner to break an existing bond with. The search for partners is performed over all beads in the reactive group and each bond break rule is tested in succession. The test of rules is done in the order they are specified, and if more than one rule match the same bead pair, the last matching rule applies. For each bead pair and bond breakage rule, it is tested if the bond between them has the specified type, and if they are further apart than the minimum bond breakage distance. Of all the potential bond breakage partners, the partner most distant in the same simulation domain (if any) is nominated for bond breakage. Bond conversion is internally represented as a bond pair that nominates each other for a bond breakage and creation of the new bond. Hence bond conversion over rules both bond breakage and creation in case they occur simultaneously.
4. Communication. The nominated partners are distributed to and aggregated across neighboring simulation domains and the closest partner is chosen for creation and the most distant partner is chosen for bond breakage. Information about which rule lead the nomination of each partner are also distributed along with a random number for stochastic bond breakage and a random number for stochastic bond creation.
5. Bond breakage. If any killbond rules are defined, all beads check, if they are part of a bond longer than the cut-off distance, and if that is the case then the bond is marked for removal. If two bonds nominate each other as bond breakage partners, then bond breakage is attempted. Each bead contributes a uniform random number for bond breakage, these are averaged and compared to the specified bond breakage probability. In case the random number is smaller than the probability, the bond is marked for removal. This ensures that beads on different simulation domains make the same random choice. When bonds are marked for removal the bond type in the corresponding entry in the bond interaction tables is set to $-1$. If a maximum rule applies to that particular bond and bead type, the table of bead functionalities is also updated. The outdated neighbor structure is retained.
6. Removing angular and dihedral interactions. To ensure parallelism, each reactive bead is alone responsible for all its angular and dihedral interactions. If a bond has been broken in its local neighborhood, the bead has to remove any angular and dihedral interactions involving that bond. This is done by generating all non-cyclic paths of length three and four either starting at or crossing the present bead using the outdated neighbor structure (which still contains the broken bonds). The beads check each path for bond breakage events (using the bond interaction tables, which shows if a bond has been marked for breakage). If a path involves a broken bond, then the bead removes the corresponding entry in its angular and dihedral interaction tables, if they exist.
7. The LAMMPS neighbor structure is updated, and the broken bond entries are removed from the bond interaction tables. If no bonds are to be created, we can jump directly to 10.
8. Bond creation. If two bonds nominate each other as bond creation partners, then an attempt is made at creating the bond. Each bead contributes a uniform random number for bond creation, these are averaged and compared to the specified bond creation probability. Again this ensures the same random choice for beads residing in different simulation domains. The new bond is added to the bond interaction table for the bead. The neighbor structure is also updated. If a maximum rule applies to the bond and bead type, the table of bead functionalities is also updated.
9. Creating angular and dihedral interactions. Again each reactive bead is responsible for determining if a bond was created in their local neighborhood. This is done the same way as angular and dihedral interactions are removed. Since the neighbor structure now contains the new bonds, we can generate non-cyclic paths of length three and four starting at or crossing the present bead using the updated neighbor structure (which now contains the new bonds). Each path is checked for bond creation events using the bond interaction tables. If the bead determines that it is part of a new triplet or quartet of beads, then it compares the bead types and directional bond types with all the angular and dihedral creation rules. If a match is found, then the bead adds the corresponding interaction to its interaction table.
10. Statistics. Distribution of statistics of the total number of bonds, angles, dihedrals introduced and removed in the current time step.

Since bond creation requires a distance check, the LAMMPS pair communication distance should be at least the longest reaction distance, otherwise bonds will only be created between bead pairs within the communication distance from each other. Since the implementation also depends on all beads knowing about all their

bonded, angular, and dihedral interactions, it will not work without Newton's 3rd law being disabled for bonded interactions. This is also required for the implementation of directional bonds. The dynamic bonding framework transparently handles symmetric bonds, hence they are just special cases of directional bonds.

The dynamic bonding code is optimized to the situation, where the density of reacting beads is so low that at most one bond breakage and bond creation event is likely to occur per bead per time step. For instance, the match making algorithm does not attempt to make matches between rejected partners, that could still be eligible for bond breakage or bond creation rules. Nor does the match making algorithm attempt to pick the most likely of multiple possible reaction path ways. For instance, if multiple bond creation rules apply to a single bead, then only the last nominated bond creation partner is stored. Hence a creation rule with a low reaction probability can overwrite the bonding partner nominated by a prior creation rule with much higher reaction probability. In this case, the high probability reaction will never happen. Similar issues apply when multiple bond break rules involve the same bead. Since the bond conversion rules are implemented as bond deletion followed by bond creation, these can interfere with both bond creation and bond breakage rules. Killbond rules are completely safe, since they are not implemented using the match making algorithm. For the DNA model, none of these caveats apply.

## References


[1] A.R. Leach, Molecular Modelling, Prentice Hall, 2001.
[2] D. Frenkel, B. Smit, Understanding Molecular Simulation: From Algorithms to Applications, vol. 1, Academic Press, 2002.
[3] A.C.T. Van Duin, S. Dasgupta, F. Lorant, W.A. Goddard III, ReaxFF: a reactive force field for hydrocarbons, J. Phys. Chem. A 105 (2001) 9396.
[4] D.G. Pettifor, New many-body potential for the bond order, Phys. Rev. Lett. 63 (22) (1989) 2480.
[5] A. Rosa, R. Everaers, J. Chem. Phys. 136 (2012) 014902.
[6] D.A. Case, T.A. Darden, T.E. Cheatham III, C.L. Simmerling, J. Wang, R.E. Duke, R. Luo, R.C. Walker, W. Zhang, K.M. Merz, et al., Amber 11, University of California, San Francisco, 2010.
[7] T.E. Cheatham III, M.A. Young, Biopolymers 56 (4) (2000) 232.
[8] B.R. Brooks, C.L. Brooks III, A.D. Mackerell Jr., L. Nilsson, R.J. Petrella, B. Roux, Y. Won, G. Archontis, C. Bartels, S. Boresch, A. Caflisch, L. Caves, Q. Cui, A.R. Dinner, M. Feig, S. Fischer, J. Gao, M. Hodoscek, W. Im, K. Kuczera, T. Lazaridis, J. Ma, V. Ovchinnikov, E. Paci, R.W. Pastor, C.B. Post, J.Z. Pu, M. Schaefer, B. Tidor, R.M. Venable, H.L. Woodcock, X. Wu, W. Yang, D.M. York, M. Karplus, CHARMM: the biomolecular simulation program, J. Comput. Phys. 30 (2009) 1545.
[9] A.D. MacKerell Jr., N. Banavali, N. Foloppe, Biopolymers 56 (2000) 257.
[10] F. Müller-Plathe, Chem. Phys. Chem. 3 (2002) 754.
[11] S.O. Nielsen, C.F. Lopez, G. Srinivas, M.L. Klein, J. Phys. Condens. Matter 16 (2004) R481.
[12] J. Langowski, Eur. Phys. J. E Soft Matter 19 (2006) 241.
[13] J.J. de Pablo, Annu. Rev. Phys. Chem. 62 (2011) 555.
[14] T.A. Knotts, N. Rathore, D.C. Schwartz, J.J. de Pablo, J. Chem. Phys. 126 (2007) 084901.
[15] E.J. Sambriski, D.C. Schwartz, J.J. de Pablo, Biophys. J. 96 (2009) 1675.
[16] E.J. Sambriski, V. Ortiz, J.J. de Pablo, J. Phys. Condens. Matter 21 (2009) 034105.
[17] A.-M. Florescu, M. Joyeux, J. Phys. Chem. 135 (2011) 085105.
[18] G.S. Freeman, D.M. Hinckley, J.J. de Pablo, J. Chem. Phys. 135 (2011) 165104.
[19] M.C. Linak, R. Tourdot, K.D. Dorfman, J. Chem. Phys. 135 (2011) 205102.
[20] K. Drukker, G.C. Schatz, J. Phys. Chem. B 104 (2000) 6108.
[21] M. Kenward, D.K. Dorfman, J. Chem. Phys. 130 (2009) 095101.
[22] T.E. Ouldridge, A.A. Louis, J.P.K. Doye, Phys. Rev. Lett. 104 (2010) 178101.
[23] M.C. Linak, K.D. Dorfman, J. Chem. Phys. 133 (2010) 125101.
[24] T.E. Ouldridge, A.A. Louis, J.P.K. Doye, J. Chem. Phys. 134 (2011) 085101.
[25] A. Savelyev, G.A. Papoian, Proc. Natl. Acad. Sci. USA 107 (2010) 20340.
[26] A. Savelyev, Phys. Chem. Chem. Phys. 14 (2012) 2250.
[27] F. Trovato, V. Tozzini, J. Phys. Chem. B 112 (2008) 13197.
[28] B. Mergell, M.R. Ejtehadi, R. Everaers, Phys. Rev. E 68 (2003) 021911.
[29] N.B. Becker, R. Everaers, Phys. Rev. E 76 (2007) 021923.
[30] M.E. Leunissen, D. Frenkel, J. Chem. Phys. 134 (2011) 084702.
[31] C.W. Hsu, F. Sciortino, F.W. Starr, Phys. Rev. Lett. 105 (2010) 55502.
[32] F.J. Martinez-Veracoechea, B.M. Mladek, A.V. Tkachenko, D. Frenkel, Phys. Rev. Lett. 107 (2011) 045902.
[33] D. Poland, H.A. Scheraga, J. Chem. Phys. 45 (1966) 1456.
[34] D. Jost, R. Everaers, Biophys. J. 96 (2009) 1056.
[35] M. Peyrard, S. Cuesta-Lopez, G. James, Nonlinearity 21 (2008) T91.
[36] D. Jost, R. Everaers, Phys. Rev. E 75 (2007) 041918.
[37] D. Jost, R. Everaers, J. Chem. Phys. 132 (2010) 095101.
[38] S. Plimpton, J. Comp. Phys. 117 (1995) 1, http://lammps.sandia.gov.
[39] P.J. Hoogerbrugge, J. Koelman, Europhys. Lett. 19 (1992) 155.
[40] P. Espanol, P. Warren, Europhys. Lett. 30 (1995) 191.
[41] S. Cocco, J.F. Marko, R. Monasson, C. R. Phys. 3 (2002) 569.
[42] R. Owczarzy, P.M. Vallone, F.J. Gallo, T.M. Paner, M.J. Lane, A.S. Benight, Biopolymers 44 (1997) 217.
[43] Y. Zeng, A. Montrichok, G. Zocchi, Phys. Rev. Lett. 91 (2003) 148101.
[44] R. Metzler, T. Ambjörnsson, J. Biol. Phys. 31 (2005) 339.
[45] Z. Rapti, A. Smerzi, K.Ø. Rasmussen, A.R. Bishop, C.H. Choi, A. Usheva, Europhys. Lett. 74 (2006) 540.
[46] T. Ambjörnsson, S. Banik, M. Lomholt, R. Metzler, Phys. Rev. E 75 (2007) 021908.